Solution Structure of Mesobilirubin XIIIα Bridged Between the Propionic Acid Substituents[a] [1]

Joaquim Crusats, Ana Delgado, Joan-Anton Farrera, Raimon Rubires,
and **Josep M. Ribó**[*]

Departament de Química Orgànica, Universitat de Barcelona, E-08028 Barcelona, Spain

Summary. The effect of cyclization of the propionic acid residues in mesobilirubin XIIIα propan-1,3-diyl ester on the angle between the dipyrrinone halves has been studied. This compound is shown to dimerize in chloroform solutions, and a conformation is proposed which is similar to that of the corresponding dimethyl ester. The results point to the contribution of π–π interactions, besides hydrogen bonding, to the geometry of the dimer.

Keywords. Bile pigments; Exciton coupling; Hydrogen bonds; π-Stacking.

Zur Struktur des über die Propionsäurereste überbrückten Mesobilirubin XIIIα in Lösung

Zusammenfassung. Es wird der Einfluß der Zyklisierung von Mesobilirubin XIIIα – Propan-1,3-diylester über die Propionsäurereste auf den Winkel zwischen den beiden Dipyrrinonhälften untersucht. Die Verbindung liegt in CHCl$_3$ als Dimeres vor. Eine Konformation analog zum entsprechenden Dimethylester wird vorgeschlagen. Neben H-Brücken sind offenbar auch π–π-Wechselwirkungen für die Struktur des Dimeren ausschlaggebend.
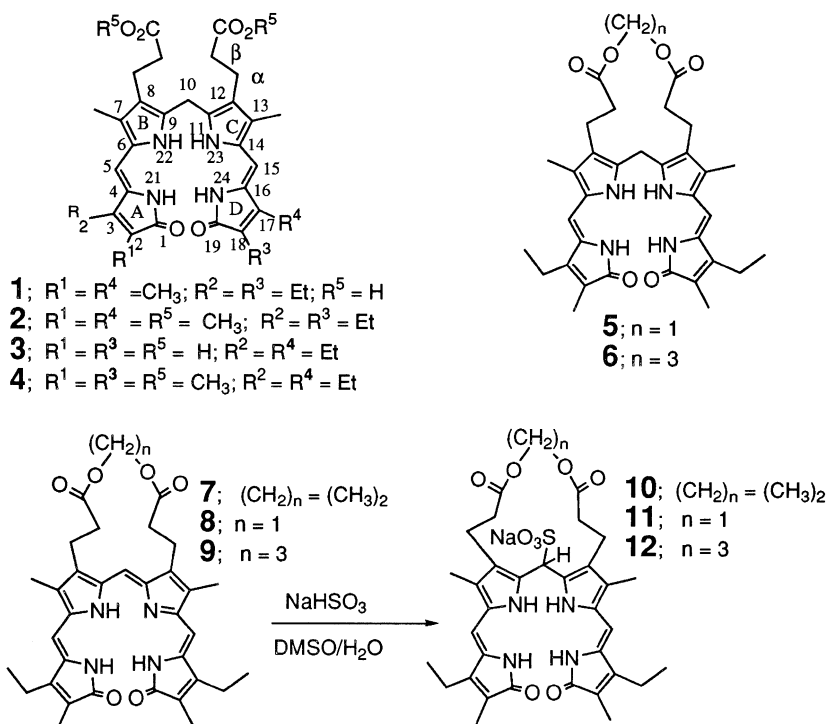
Introduction

Biliverdins (bilin-1,19-diones) of the natural series IXα [2] can be internally cyclized between the propionic acid chains by formation of the diester of a short chain α-ω-alkanediol [3]. In a previous work [1] we have studied the effect of this bridging on the helix conformation of biliverdins. The reduction of biliverdins to bilirubins for preparative purposes is easily accomplished using NaBH$_4$ in methanol. Thus, bilirubins cyclized between the propionic acid chains can be obtained from the corresponding biliverdins; the propan-1,3-diyl diester of mesobiliverdin XIIIα (**9**), for example, affords the corresponding bilirubin diester (**6**). However, the methylene diesters of biliverdins (*e.g.* **8**) give hydroxyacids upon reduction with NaBH$_4$ and the corresponding methylene diester (**5**) cannot be obtained [4]. This is probably due to the inductive effect of the two methylenic

---

[a] In memory of *Francesc R. Trull* who dedicated many years of his life to bilirubin chemistry
[*] Corresponding author

oxygens on the carbonyl groups [5]. However, this partial reduction could also be a consequence of a strong torsional effect exerted by the bridge. Here we report results which should help to clarify this point.

1; $R^1 = R^4 = CH_3$; $R^2 = R^3 = Et$; $R^5 = H$
2; $R^1 = R^4 = R^5 = CH_3$; $R^2 = R^3 = Et$
3; $R^1 = R^3 = R^5 = H$; $R^2 = R^4 = Et$
4; $R^1 = R^3 = R^5 = CH_3$; $R^2 = R^4 = Et$

5; n = 1
6; n = 3

7; $(CH_2)_n = (CH_3)_2$
8; n = 1
9; n = 3

10; $(CH_2)_n = (CH_3)_2$
11; n = 1
12; n = 3

NaHSO$_3$

DMSO/H$_2$O

Bilirubins (biladiene-*ac*-1,19-diones, [2]) with free carboxylic acid groups at C8 and C12 are monomeric in chloroform and dimethyl sulfoxide solutions [6] and their structure corresponds to the so-called ridge-tile conformation (Scheme 1) with the NH of the dipyrrinone halves *anti* to each other. This structure is stabilized by intramolecular hydrogen bonds between the carboxylic acid groups and the lactam and pyrrolic NH. In dimethyl sulfoxide the structure is similar to that in chloroform, but solvent molecules are included in the hydrogen bond matrix.
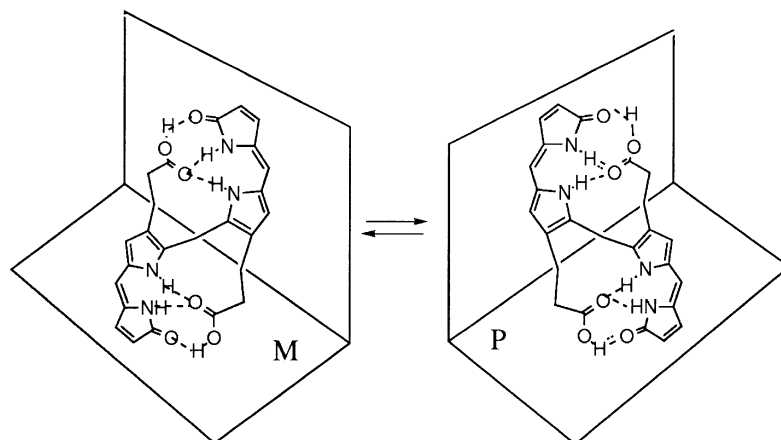
Scheme 1

Bilirubin dimethyl esters show a dimerization equilibrium [7] whose solvent dependence points to intermolecular hydrogen bonding. Probably these hydrogen bonds occur *via* dipyrrinone-dipyrrinone interactions [6, 7]. Here we present results on the homoassociation of a bridged cyclic diester which allow the inference of more details on the solution structure of bilirubin esters or non-propionate substituted bilirubins.

Results and Discussion

Vapor osmometry measurements (Table 1) show that in chloroform solutions the cyclic ester **6** as well the dimethyl ester of mesobilirubin XIIIα (**4**) have apparent molecular masses twice the calculated mass. Furthermore, they show a low concentration dependence (measured range: $6 \cdot 10^{-3}$–$3 \cdot 10^{-2}$ molal). In the case of the dimethyl ester of similar bilirubins, this has been previously reported for non polar aprotic solvents [7a]. The osmotic coefficients ($\Phi = MW_{calc}/MW_{exp}$) are equal for **4** and **6**, suggesting that the ester groups do not play a significant role in the interactions which perform the biladiene-*ac* dimerization. These results also indicate a higher degree of homoassociation for **4** and **6** than for the dimethyl ester of mesobilirubin IXα (**2**). This agrees with previous results on the effect of the *exo* vinyl groups on the intramolecular hydrogen bonding of bilirubins [8]. Assuming that dimerization occurs through planar antiparallel intermolecular hydrogen bonding of the dipyrrinone halves [9], the non-bonding interactions between the *exo* substituents (at C2 or C18) of one dipyrrinone with the pyrrole ring of the second dipyrrinone should be higher for a vinyl or an ethyl group at C2 (series IIIα and IXα) than for a methyl group (series XIIIα).

UV/Vis Absorption Spectra

The changes induced by the solvent in the UV/Vis spectra of bilirubins have been extensively investigated [6, 7]. The bilirubin spectrum is due to two identical or very similar chromophores (dipyrrinones), and the visible absorption spectra correspond to the superposition of two absorption bands of different intensities separated by about $2000 \pm 500 \, cm^{-1}$. *Lightner* has shown that the exciton coupling model correlates well the visible absorption spectra of bilirubins with the relative spatial position of their dipyrrinone halves [10]. However, this model should be

Table 1. Vapour pressure osmometry results (osmotic coefficients Φ) of $2.5 \cdot 10^{-2}$ molal solutions in CHCl$_3$; Φ values show only small changes in the concentration range of $3 \cdot 10^{-2}$–$6 \cdot 10^{-3}$ molal solutions

	$\Phi(MW_{calc}/MW_{exp})$
2	0.65 ± 0.02
4	0.50 ± 0.02
6	0.50 ± 0.02
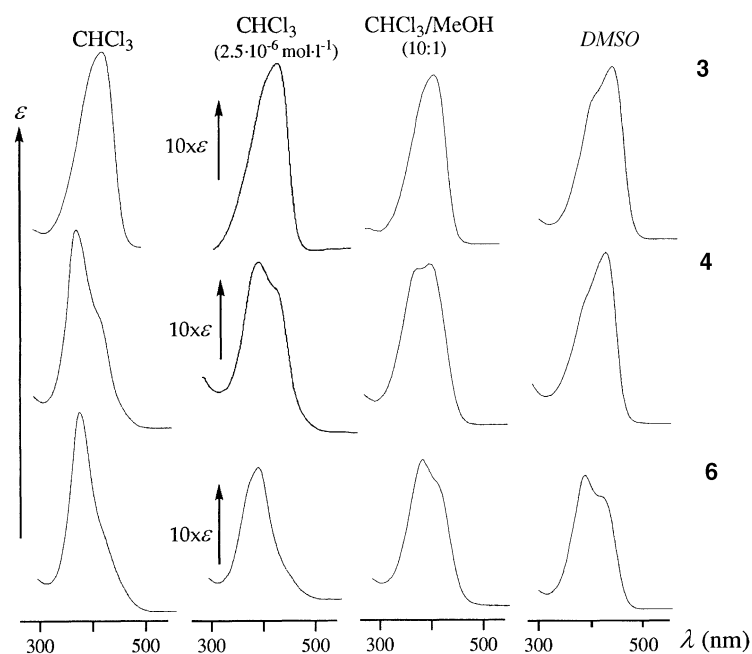
Fig. 1. Visible absorption spectra of mesobilirubins $(2.5 \cdot 10^{-5} \, \mathrm{mol} \, \mathrm{l}^{-1})$

Table 2. UV/Vis absorption spectra of bilirubins **3**, **4**, and **6**; ε values are calculated for monomers

	Solvent	Concentration	$\lambda_{max}(\varepsilon)(\mathrm{nm}(\mathrm{mol}^{-1} \cdot 1 \cdot \mathrm{cm}^{-1}))$
3	CHCl$_3$	[a]	432 (53000)
	CHCl$_3$/MeOH[b]	[a]	432 (53000)
	DMSO	[a]	386sh (46000), 426 (60000)
4	CHCl$_3$	$2.5 \cdot 10^{-5}$	378 (58000), 418sh (33000)
	CHCl$_3$	$2.5 \cdot 10^{-6}$	386, 410sh (1.2:1.0)
	CHCl$_3$/MeOH[b]	[a]	394, 416 (1:1)
	DMSO	[a]	380sh (47000), 427 (65000)
6	CHCl$_3$	$2.5 \cdot 10^{-5}$	373 (55000), 420sh (14000)
	CHCl$_3$	$2.5 \cdot 10^{-6}$	389 (43000), 440sh (13000)
	CHCl$_3$/MeOH[b]	[a]	370, 414 (1.2:1)
	DMSO	[a]	388 (56000), 418 (47000)

[a] Concentration independent; (measured at $2.5 \cdot 10^{-5}$ and $2.5 \cdot 10^{-6} \, \mathrm{mol} \cdot 1^{-1}$); [b] 10:1

applied only to the monomers of biladienes-*ac*, because the homoassociation causes additional intermolecular perturbations between the chromophores [9].

Figure 1 and Table 2 show the visible absorption spectra of **6** compared to those of **3** and **4**. The concentration dependence of the spectral pattern can be attributed to the presence of a monomer-dimer equilibrium; a similar dependence is detected for chloroform solutions of bilirubin esters. In this respect, Fig. 1 shows in the case of **3** the well known fact that for free carboxylic acid bilirubins there are no significant changes between chloroform at several concentrations, chloroform/ methanol, and dimethyl sulfoxide, which demonstrates its presence as a monomer.

3 occurs as a monomer in dimethyl sulfoxide and in chloroform. In *DMSO*, its UV/Vis spectrum is similar to that in chloroform, but the shoulder at lower wavelengths shows a small increase in its relative intensity. According to the exciton coupling model, this difference indicates smaller angles between the dipyrrinone planes in *DMSO* than in CHCl$_3$. This suggests that the previously reported [11] inclusion of *DMSO* molecules in the hydrogen bond matrix of the ridge-tile conformation results in an increase of the distances in the associated system carboxylate-dipyrrinone and a decrease of the angle between the dipyrrinone planes. We discuss below the expected changes of the relative intensities of the absorption bands with the relative position of both dipyrrinone halves.

In the case of chloroform, the concentration dependence and the pattern change observed by addition of methanol show the prevalence of the dimer in concentrated chloroform solutions and of the monomer in dilute chloroform/methanol solutions. **4** exhibits differences between the spectra in *DMSO* and in chloroform/methanol; the relative intensity of the high energy absorption band is lower in *DMSO* than in chloroform/methanol. This could be attributed to the residual presence of dimers in chloroform/methanol (10:1) or to conformational changes at C5, C10, or C15 originating from solvent effects. **6** shows the same spectral pattern in chloroform/ methanol and in *DMSO*. Assuming that in *DMSO* homoassociation does not occur, the angle between the dipyrrinone halves in the monomer must be different for **4** and **6**.

According to the exciton coupling model applied to bilirubins [10], in *DMSO* monomeric **4** would show an angle between the dipyrrinone planes higher than 90° (the α state being the state at lower energies [10]; $\varepsilon^\alpha/\varepsilon^\beta > 1$) and **6** a corresponding angle smaller than 90° ($\varepsilon^\alpha/\varepsilon^\beta < 1$). This is a reasonable conclusion, because of the torsion effect of the bridge cycle would force narrower dihedral angles for **6** than for the open chain diester **4**.

The intensity ratio of these two bands is a sensitive parameter for the angle between the transition dipole moments of both chromophores, *i.e.* between the two dipyrrinone planes.

For this discussion, the planarity between the rings of the (*Z*)-*syn* system lactam-pyrrole is assumed as an approximation. In the ridge-tile conformation, the angle between the transition dipole moments of both chromophore depends on the dihedral angle around C10, but also on the dihedral angles around C5 and C15. If the dihedral angle C4-C5-C6-N22 and C9-C10-C11-N23 are of the same sign as the bilirubin helix (*e.g.* (*P*), +, +), there is an increase in the dihedral angle of the transition dipole moments; angles of different sign (*e.g.* (*M*), +, +) result in smaller angles.

Figure 2 shows the intensity ratio (oscillator strengths ratio) between bands calculated by the CIS method from *ab initio* calculations (Gaussian 94) using the 3-21G basis set (see Experimental for details) and compared to the values obtained from the exciton coupling model using standard internal geometries. Significant differences between both models are found when the distances between the π systems of both dipyrrinones decreases, *i.e.* when perturbation increases. This is the case when the distances between the pyrrolic systems decrease at high dihedral angle values of N22-C9-C10-C11 and C9-C10-C11-N23, or when these dihedral angles are of different sign, *e.g.* 60°/−60°. For these situations, the differences between the CIS calculations using 3-21G or 6-31G* basis sets are also significant. Further, for these cases, and especially for the conformations 60°/−60° (*syn* between the pyrrolic NHs), significant changes would be expected for the
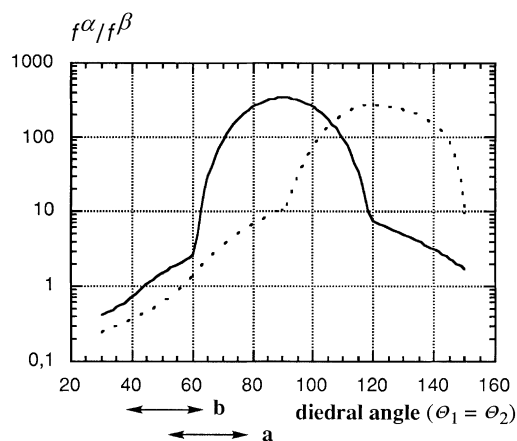
$$f^{\alpha}/f^{\beta}$$

Fig. 2. Dependence of the oscillator strength ratio ($\mathbf{f}^{\alpha}/\mathbf{f}^{\beta}$; bands α and β correspond to the low and the high energy absorption, respectively) upon the dihedral angle (N22-C9-C10-C11 (Θ_1) and C9-C10-C11-N23 (Θ_2)) for biladienes-*ac*; calculated from a) the exciton coupling model, b) single CI from *ab initio* 3–21G basis set calculations; symbol $\leftrightarrow$ corresponds to the estimated practical range where two absorption bands could be differentiated

absorption spectrum which accounts for an *anti* conformation of both dipyrrinones. In the case of dihedral angles of the same sign (pyrrolic NHs in *anti* conformation) and values in the range between 30° and 60°, the differences between both methods are small (*ca.* 10° for the same intensity ratio), and the CIS results do not differ significantly using 3-21G or 6-31G* basis sets. The experimental difficulties which obviously occur for the detection of two bands in the case of high or small ratios (*e.g.* higher than 3 or lower than 0.3) restrict the usefulness of the relative intensities approach to angle ranges between transition dipole moments (*i.e.* between dipyrrinone planes) around 90°. Nevertheless, for bilirubins only conformational changes in this range should be expected. Force field calculations (see Experimental and Ref. [12]) also show that the more stable conformations of biladienes-*ac* correspond to both dipyrrinones in a *synclinal* conformation (dihedral angles at C10 of the same sign and *Ca.* 60°). The geometry optimization of biladiene-*ac* models using *ab initio* methods and the 6-31G* basis set give an energy minimum with dihedral angles around C9–C10 and C10–C11 not different from that obtained using force field methods. They correspond to angles of approximately 100–110° between the transition dipole moments of both chromophores. Taking into account that the experimental ratio of intensities of the visible absorption bands in *DMSO* of **4** and **6** changes from ≈ 2 to 0.5 (see Fig. 2), both monomers show dihedral angles around C10 in the region of 50°, differing 20°–10° ($\approx 60°$ for **4** and $\approx 40°$ for **6**). Thus, the transition dipole moments of both dipyrrinones change from $>90°$ to $<90°$.

Visible spectra of cyclized bilirubinoids (biliverdin bisulfite adducts)

Biliverdins add nucleophilic reagents at the carbon atom 10 giving biladienes-*ac*. The formation of the adducts could be followed *via* the visible spectra which
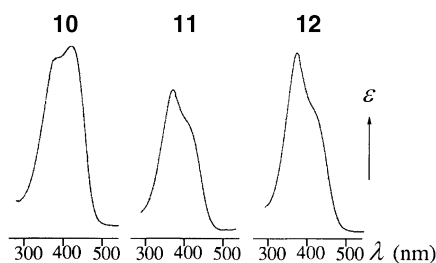
Fig. 3. Visible absorption spectra of bilirubinoids **10**, **11**, and **12** obtained by the reaction of the corresponding biliverdins $(2.5 \cdot 10^{-6}\,\mathrm{mol} \cdot \mathrm{l}^{-1}$ *DMSO*/H$_2$O (1:1)) with NaHSO$_3$/Na$_2$SO$_3$ $(0.05\,\mathrm{mol} \cdot \mathrm{l}^{-1}$ ($pH \approx 7$))

changed from the mesobiliverdin absorption pattern (blue-green) to the mesobilirubin one (yellow). **7** and **9** added bisulfite in *DMSO*/water solutions giving bilirubinoids (**10** and **13**) with similar visible absorption spectra as the corresponding bilirubins (see Fig. 3). Consequently these results point to similar structures for the bilirubinoids and the corresponding bilirubins.

8 also added bisulfite giving the corresponding bilirubinoid **11** which showed a similar spectrum to **13** and **6**. These results demonstrate that the smaller cycle of the methylene diester affects the structure in the solution of the bilirubin derivative in a similar degree to the propan-1,3-diyl ester. Furthermore, this shows that the methylene bilirubin diesters cannot be obtained by reduction of the corresponding biliverdins [4, 5] because of the activating effect exerted by the methylene oxygen on the carbonyl group and not to torsional energy effects which could affect the addition of nucleophiles at C10.

Luminescence spectra

The monomers (*DMSO* solutions) of the dimethyl ester **2** and the cyclic ester **6** showed fluorescence yields of the same order of magnitude (see Table 3). These similar fluorescence yields point to similar deactivation pathways. This implies that the deactivation pathways by rotation around C10 do not play a significant role. Such a rotation is not possible for **6**.

Table 3. Fluorescence of bilirubins **1**, **2**, and **6** at $1.3 \cdot 10^{-5}\,\mathrm{mol} \cdot \mathrm{l}^{-1}$ in *DMSO* and CHCl$_3$ (see Experimental)

	DMSO			CHCl$_3$		
	λ (nm) excitation	λ (nm) emission	Relative quantum yields[b]	λ (nm) excitation[a]	λ (nm) emission	Relative quantum yields[b]
1	460$_{max}$	n.d.	$< 1\ 10^{-8}$	452$_{max}$	517	$(1.6 \pm 0.3) \cdot 10^{-6}$
2	426$_{max}$	475	$(2.8 \pm 0.3) \cdot 10^{-5}$	382$_{max}$	466	$(1.7 \pm 0.3) \cdot 10^{-5}$
	400$_{sh}$	475	$(2.1 \pm 0.3) \cdot 10^{-5}$	414$_{sh}$	466	$(3.5 \pm 0.3) \cdot 10^{-5}$
6	386$_{max}$	480	$(1.8 \pm 0.3) \cdot 10^{-5}$	384$_{max}$	539	$(2.3 \pm 0.3) \cdot 10^{-5}$
	416$_{sh}$	480	$(2.1 \pm 0.3) \cdot 10^{-5}$	420$_{sh}$	539	$(3.5 \pm 0.3) \cdot 10^{-5}$

[a] Corresponding to the peak maximum and the shoulder of the absorption spectra; [b] relative to ε of the excitation wavelength and assuming that only the monomer is present

The free bilirubins showed lower fluorescence than the esters; in fact, the monomer in *DMSO* did not show any detectable luminescence. This could be due to the previously reported inclusion of *DMSO* between the carboxylate and the dipyrrinone NHs, which would imply an effective deactivation of the excited state.

In the case of the dimers (chloroform solutions) of the diesters, the fluorescence spectra demonstrated the heterogeneity of the absorption bands. The relative luminescence yield was significantly higher by excitation at the shoulder at low energies than by excitation at the peak maximum (Table 3), but the fluorescence emission was the same for both excitations. Assuming that the absorption spectrum corresponded in part to the dimer (toward higher energies), and in part to the monomer (principally located in the shoulder at lower energies), these results suggest that only the fluorescence corresponding to the monomer is being detected and that the photoexcitation of the dimer results in the splitting to the monomers ($BR-BR^* \rightarrow BR^* + BR$). This would account for the observed differences of quantum yield. However, more experiments have to be performed before an explanation of to these results can be given.

^1H-NMR Spectra

ROESY experiments confirmed the (*Z*)-*syn* structures around C5 and C15; the NOEs expected for these structures were detected (Table 4). This was true for all monomers (*DMSO*-d_6) and homoassociates (CDCl$_3$). The bilirubin esters showed NOEs in CDCl$_3$ which confirmed the presence of homoassociation (Table 4).

Table 4. NOE signals (300 MHz, ROESY, $t = 600$ ms, $1 \cdot 10^{-3}$ mol $\cdot$ l^{-1}) of the monomer (*DMSO*-d_6) an dimer (CDCl$_3$) of some bilirubins; signs indicate the relative intensity order from very intense (+++) to very weak (+) and 0 (not detected)

	Solvent	Z-*syn*				Conformation at C10			Homoassociation				
		a	b	c	d	e	f	g	h	i	j	k	l
4	CDCl$_3$	(+++)	(+++)	(++)	(++)	(++)	(+++)	(++)	(++)	(++)	(++)	(+)	0
6	CDCl$_3$	(+++)	(+++)	(++)	(++)	0	(++)	0	(++)	(++)	(++)	0	0
3	CDCl$_3$	(+++)	(+++)	(++)	(++)	(++)	(++)	0	0	0	0	0	0
4	DMSO	(+++)	(+++)	(++)	(++)	(++)	(++)	0	0	0	0	0	0
6	DMSO	(+++)	(+++)	(+)	(++)	(++)	(++)	(+)	0	0	0	0	0
3	DMSO	(+++)	(+++)	(++)	(++)	(+)	0	0	0	0	0	0	0

(Z)-syn   C10   Dimerization
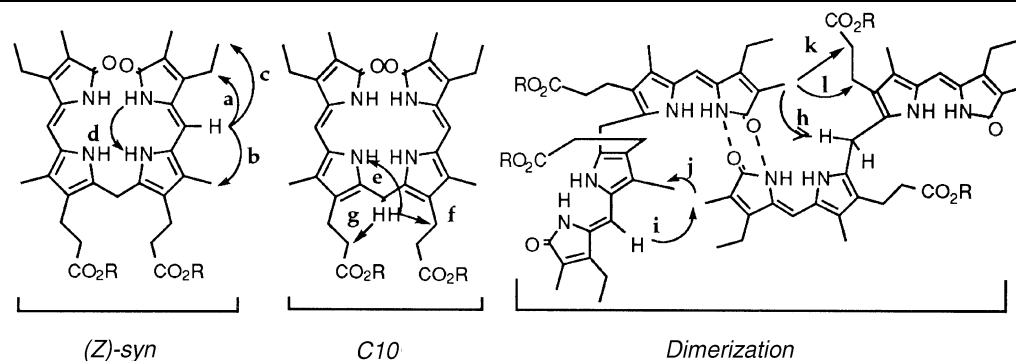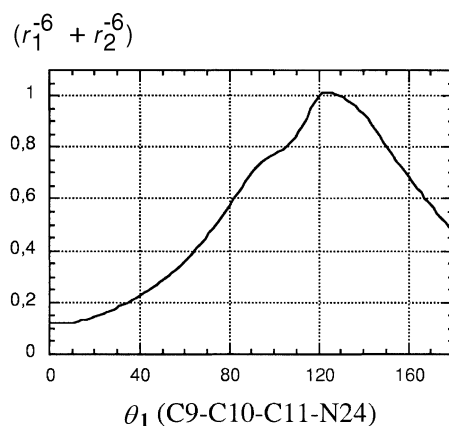
$$(r_1^{-6} + r_2^{-6})$$

Fig. 4. Variation of $(r_1^{-6} + r_2^{-6})$ with the diedral angle Θ_1 (C9-C10-C11-N24) in bilirubins; r_1 and r_2 are the distances between the H at N24 and the protons at C10

Monomers. With respect to the conformations around C10, the NOE between the methylene protons at C10 and the pyrrolic NHs could be used as a monitor of the dihedral angles around C10. However, these NOEs involve a system higher than two spins (H-C10, pyrrolic NH, and the protons of the propionate chain) so that a quantitative correlation between NOE (intensities) and distances (r^{-6}) is not possible [13]. Further, a qualitative description of this NOE shows a low sensitivity to the changes on the dihedral angle. From Fig. 4 (plot of r^{-6} (r = distance from H-C10 to the pyrrolic NH) *vs*. dihedral angle (N22-C9-C10-C11), it can be seen that a detectable NOE must be expected for a wide range of dihedral angle values (distance changes between 2.9 Å and 3.5 Å), and as a consequence it is of low value for conformational analysis.

The monomers of **4** and **6** showed NOEs between the protons of the propionate chains and the protons at C10. The most significant difference between both esters was the NOE between H-C10 and the β-methylene group, which could only be detected for the cyclic ester. In the open chain diester, *antiperiplanar* conformations for the propionate chains can be expected, implying greater distances between the protons at βC and C10 than for the cyclic ester.

The spin system $-CH_2-CH_2-$ of the propionate chains is apparently an A_2X_2 (A_2M_2) system with $J \approx 8$ Hz for the monomers of **4** and **6**. This points to a conformational heterogeneity of the bridge cycle.

Dimers

Previously reported data [7] and the vapour osmometry described above show that bilirubin diesters in apolar solvents dimerize through hydrogen bonds between dipyrrinones. However, there are very few experimental results which allow a definite structure for these dimers to be suggested.

For **4** and **6** in CDCl$_3$, *i.e.* for their dimers, NOEs were detected that can only be attributed to the presence of homoassociation (see Table 4; *h*, *i*, *j*, *k*). The ROESY experiments showed similar results for both types of esters, pointing to dimers of similar geometry. However, they showed significant differences (*e*, *f*, *g*)

with respect to the conformation of the propionate chains and the conformation around C10. The small NOE (k) detected in **4**, but absent in **6**, between the β-methylene group and the methyl group at C2 (C18) could be attributed to the different conformation of the propionate chains and not to a very different geometry of the interacting dipyrrinones.

The dimer of **6**, compared to its monomer and also to **4**, showed no NOE between H-C10 and NH (e). This could be interpreted by assuming smaller dihedral angle values around C10 (N22-C9-C10-C11 and C9-C10-C11-N23) for the dimer of **6** than for the corresponding monomer and the dimer of **4**. The absence of NOE between the β-methylene and H-C10 compared to the monomer (see Table 4; g) could be a consequence of the effect exerted in the bridge cycle by the decrease of the angle between the dipyrrinone planes. The dimerization of **4** results in an increase of the NOE between H-C10 and the methylene groups (f, g), which could also be explained by a decrease in the angle between the dipyrrinone planes. In this case, in the absence of an internal cycle, a decrease in the angle between the dipyrrinone planes would result in a decrease in the distances between H-C10 and the protons of the propionate chains.

Molecular models using force field methods (see Experimental) afford structures in agreement with the former results. These calculations suggest an open *synclinal* conformation for the CH_2-CH_2 chain of **6**; the structure shown in Fig. 5 corresponds to this conformation.

The effect exerted on the propionate chains of **6** by dimerization exerts dramatic effects on the CH_2-CH_2 spin system; in the monomers of **4**, **6**, and the dimer of **4**, this spin system was detected as an A_2X_2 (A_2M_2) system. This points to the conformational heterogeneity of the propionate substituents. However, the dimer of **6** showed a AA'XX' (AA'MM') system, whose pattern and coupling constant values are not significantly different from those previously reported for the same spin system in the methylene diesters of bilin-1,19-diones (biliverdins) [1]. This points to a unique bridge cycle conformation. The fast exchange rate between the hydrogen bonded dimers would result in the detection of an AA'XX' spin system instead of the expected ABXY system. Furthermore, the coupling constant values of this AA'XX' system ($J_{AA'} \approx J_{XX'} = 14–17\,Hz$; $J_{AX} = 8–10\,Hz$, $J_{AX'} = 2–3\,Hz$) can only be attributed to a closed *antiperiplanar* (160°–140°) or open *synclinal* (80–100°) conformation of the carbon chain. For a more detailed discussion, see Ref. [1].

On the structure of the dimers

According to these and previously reported results (see *e.g.* Ref. [12]) we can assume a *(Z)-Syn* structure around C5(C15) for biladienes-*ac* and an alternated conformation around C10 with dihedral angles (N23-C9-C10-C11 and C9-C10-C11-N24) of the same sign. Otherwise, there are destabilizing non-bonding interactions.

Most of the NOEs due to homoassociation point to antiparallel hydrogen bonding between dipyrrinones, especially the NOE between the methyl group at C2 (C18) and H-C10 (h, Table 4). The NOE of this methyl group with the vinylic proton at C5 (C15) (i) could be attributed to the interaction between two non-direct
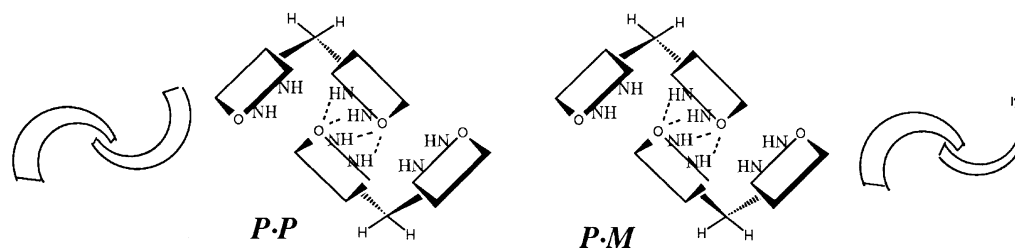
Scheme 2

hydrogen bonded dipyrrinones. Also, some of the former NOEs could be attributed to this cross-interaction between both bilirubins.

A dimeric structure based on planar antiparallel hydrogen bonded dipyrrinones implies that for each bilirubin one non-associated dipyrrinone remains (see Scheme 2). These two terminal non-associated dipyrrinones could act as new association links affording oligomerization which, according to the vapour osmometry measurements, does not occur or only at a very low level. In consequence, the centrosymmetric (*P,M*)-dimer (see Scheme 2) could be excluded on the basis of the absence of oligomerization. The dimer with two bilirubins of the same helix sign would also allow oligomerization, but in this case the oligomerization would give higher non-bonding interactions than in the centrosymmetric dimer. Furthermore, these dimers do not explain the experimental results which show that dimerization induces conformational freezing of the bridge cycle. The two dimer structures of Scheme 2 would allow a flexibility of the bridge cycle similar to that of the monomer. When the four dipyrrinones are involved in the dimer arrangement, the interacting dipyrrinones cannot be coplanar.

The coplanar antiparallel dipyrrinone dimer can be considered as a particular case of the lactam-lactam interaction [14] with additional intermolecular hydrogen bonding between lactam and pyrrilic NHs. However, the dipyrrinone has a π electron system, which in contrast to the currently studied saturated lactams, could give π–π interactions. In fact, Density Functional Theory (DFT) calculations with geometry optimization on the dimer of 5-methylen-3-pyrrolin-2-one give energy minima for the expected planar antiparallel dimer as well as for a non-planar antiparallel dimer with ≈ 60° between the cycle planes where a compromise exists between hydrogen bonding and stabilizing π–π interactions [15]. Such a type of association, *i.e.* antiparallel non-planar dipyrrinone association, could well account for the structure of the bilirubin dimer.

Figure 5 shows the dimer structure originating from the intercalation of two bilirubins of the same helix sign and intermolecular antiparallel π interaction of the two central pyrrolinones. For this type of structure, and for a separation of the π stacked ring between 2.0–2.5 Å, the distances obtained between the oxygen of the central rings and the lactam NH of the external rings are 1.7–1.5 Å, *i.e.* two additional hydrogen bonds could be formed. Dimerization through this four point chelating structure would lock the bilirubin towards less open helices, in agreement with the above reported results. In this model, the intermolecular distances between the methyl groups at C2 and H-C10 and H-C5 and the methyl group at C7 could explain the detected NOEs (*h*, *i*, *j* in Table 4). Differences between **4** and **6** would
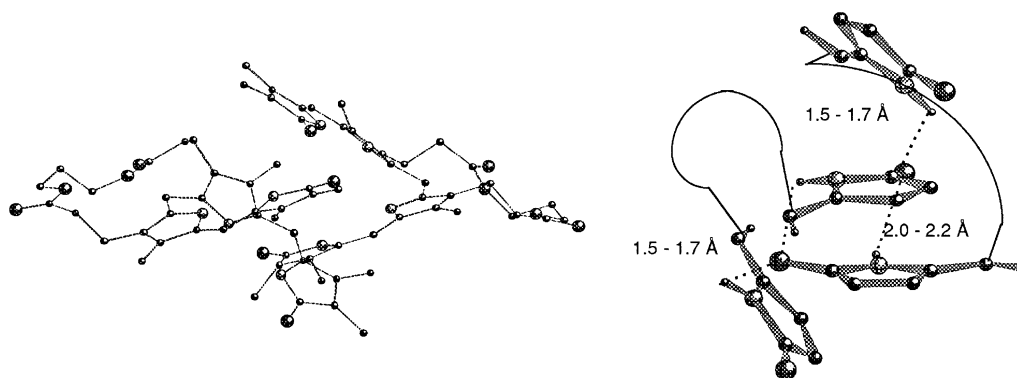
Fig. 5. Model for the dimer of **6**; on the right side, only the terminal rings are shown; ethyl groups are represented as methyl groups; protons are hidden in the figure at the left and methyl groups in the figure at the right

be located in the dihedral angles around C10, in the angle between the planes of the central pyrrolinones (both higher for the cyclic esters), and in the participation of the pyrrolic NH in the hydrogen bond matrix which, as a consequence of the more open structure, would be greater for the open chain diesters. In spite of the speculative character of this model it explains the results reported here. According to this model biladiene-*ac*-diones without free carboxylic acid groups (*e.g.* the related esters or bilirubins without propionate substituents) would associate through π interactions in addition to hydrogen bonding. In dipyrrinones, where no non-bonding interactions hindering oligomerization are present, antiparallel π stacking could occur, and this in fact has been already reported [16].

Experimental

Vapour osmometry mesurements (Table 1) were performed with a Knauer 0587 instrument in CHCl$_3$ at 40°. UV/Vis spectra (Figs. 1, 2 and Table 2) were recorded with a Perkin-Elmer Lambda 5 spectrometer. Luminescence spectra (Table 3) were recorded with an Aminco-Bowman Series 2 instrument with a Xe lamp (1.5 W). ^{1}H NMR spectra were recorded with a Varian Unity 300 (300 MHz) and ROESY experiments with a Varian Unity 500 (500 MHz) spectrometer (*TMS* as internal reference in CDCl$_3$ previously filtered through basic alumina I). The ROESY experiments (Table 4) were carried out at a spin lock time of 600 ms.

Calculations were performed with an SG MIPS R8000 computer. For force field calculations, the Universal Force Field with Charge Equilibration scheme [17] was used on the interface Cerius2 (Molecular Simulations). For *ab initio* and CIS calculations, Gaussian94 [18] was used on the Cerius 2 interface; 3-21G and 6-31G* basis set (see text). Spartan SGI 4.1.2 (Wavefunction Inc.) was used for DFT (LSDA/VWN; DN basis) calculations.

The preparation of mesobilirubin IXα (**1**) and its dimethyl ester (**2**) has been described in Ref. [19]. Mesobilirubin XIIIα (**3**) and its dimethyl ester (**4**) were obtained according to Ref. [20]. Mesobilirubin XIIIα propan-1,3-diyl diester (**6**), mesobiliverdin XIIIα dimethyl (**7**), methylene (**8**), and propan-diyl (**9**) diesters were obtained as previously described [3, 4].

Bisulfite adducts of bilirubins (**10**, **11**, **12**) were obtained by adding a 1 *M* Na$_2$SO$_3$/NaHSO$_3$ (1:1) solution ($pH \approx 7$) to a *DMSO*/water solution of the corresponding biliverdin ($2.5 \cdot 10^{-6}$ mol $\cdot$ l^{-1}). These solutions were directly used for recording their UV/Vis spectra (Table 3).

Acknowledgments

References

[1] A large part of this work corresponds to the PhD Thesis of Crusats J (1996) University of Barcelona. See former paper: Crusats J, Benitez P, Farrera J-A, Rubires R, Ribó JM (1998) Monatsh Chem **129**: 535

[2] a) IUPAC-IUB Nomenclature of tetrapyrroles (1987) Pure Appl Chem **59**: 779; b) Falk H (1989) The Chemistry of Linear Oligopyrroles and Bile Pigments. Springer, Wien New York

[3] a) Ribó JM, Crusats J, Marco M (1994) Tetrahedron **50**: 3967; b) Boiadjiev SE, Anstine DT, Lightner DA (1995) Tetrahedron Asymmetry **6**: 901

[4] Crusats J, Farrera JA, Ribó JM (1996) Monatsh Chem **127**: 85

[5] Benitez P, Delgado A, Farrera JA, Ribo JM (1997) Synth Comm **27**: 1697

[6] a) Kaplan D, Navon G (1983) Israel J Chem **23**: 177; b) Person RV, Peterson BR, Lightner DA (1994) J Am Chem Soc **116**: 42

[7] a) Falk H, Schlederer T, Wolschann P (1981) Monatsh Chem **112**: 199; b) ref. [2b] pp 323–324 and 420

[8] a) Trull FR, Ma J, Landen GL, Lightner DA (1983) Israel J Chem **23**: 211; b) Lightner DA, Trull FR (1983) Spectrosc Lett **16**: 785

[9] Falk H, Gergely S, Grubmayr K, Hofer O, Leodolter A, Neufingerl F, Ribó JM (1977) Monatsh Chem **108**: 1113

[10] See *e.g.* Lightner DA; Gawronski JK; Wijekoon WMD (1987) J Am Chem Soc **109**: 6354

[11] Dörner T, Knipp B, Lightner DA (1997) Tetrahedron **53**: 2697

[12] a) Falk H, Müller N (1983) Tetrahedron **39**: 1875; b) Boiadjiev SE, Anstine T, Lightner DA (1994) Tetrahedron Asym **5**: 1945

[13] We studied the dependence of intensity on the mixing time (ROESY) for several bile pigments. The signals show very different decays. This does not allow the application of quantitative relationships. In consequence, the results here reported have been interpreted in a semiquantitative mode in the sense of Neuhaus D, Williamson M (1989) The Nuclear Overhauser Effect in Structural and Conformational Analysis. Verlag Chemie, New York, p 95

[14] Burrows AD, Chan CW, Chowdhry MM, McGrady JE, Mingos DMP (1995) Chem Soc Rev 329

[15] These methods can only be used to estimate the presence of energy minima but not their relative energy levels because of the low reliability of the calculated hydrogen bond energies inferred from *ab initio* self-consistent functional density methods; a) Novoa, JJ, Sosa C (1995) J Phys Chem **99**: 15837; b) Hobza P, Kabelàc M, Sponer J, Mejzlic P, Vondrasek J (1997) J Comput Chem 1137

[16] Boiadjiev SE, Anstine DT, Lightner DA (1995) J Am Chem Soc **117**: 8727

[17] a) Rappe AK, Goddard III WA (1991) J Phys Chem **95**: 3358; b) Rappe AK, Casewit CJ, Colwell KS, Goddard III WA, Skiff WM (1992) J Am Chem Soc **114**: 10024

[18] Gaussian 94, Revision B. 3; Frisch MJ, Trucks GW, Schlegel HB, Gill PMW, Johnson BG, Robb MA, Cheeseman JR, Keith T, Petersson GA, Montgomery JA, Raghavachari K, Al-Laham MA, Zakrzewski VG, Ortiz JV, Foresman JB, Peng CY, Ayala PY, Chen W, Wong MW, Andres JL, Replogle ES, Gomperts R, Maartin RL, Fox DJ, Binkley JS, Defrees DJ, Baker J, Steward JP, Head-Gordon M, Gonzalez C, Pople JA (1995) Gaussian, Inc., Pittsburgh, PA

[19] McDonagh AF, Palma LA (1980) Biochem J **189**: 193

[20] a) Monti D, Manitto P (1981) Synth Comm **11**: 811; b) Ma JS, Lightner DA (1984) J Heterocyclic Chem **21**: 1005; c) Reisinger M, Trull FR, Lightner DA (1985) J Heterocyclic Chem **22**: 1221